J Appl Electrochem (2007) 37:1015–1019
DOI 10.1007/s10800-007-9342-0

ORIGINAL PAPER

Development of nickel incorporated aluminum alloy matrix as an efficient sacrificial anode

S. M. A. Shibli · V. S. Dilimon · Asha Mohan

Received: 22 November 2006 / Revised: 21 May 2007 / Accepted: 25 May 2007 / Published online: 15 June 2007
© Springer Science+Business Media B.V. 2007

Abstract Al–Zn + Ni matrix anodes were fabricated using Ni as activator. The Al–Zn + Ni anodes had good physico-chemical characteristics. Reinforcement by Ni resulted in improvement in grain size of the metal–metal matrix. The effect of Ni on the galvanic performance of the anodes was evaluated based on several electrochemical methods. Incorporation of Al–Zn anodes with Ni caused an increase in the galvanic performance. Breakdown of the passive oxide film was facilitated by the presence of nickel. The optimum Ni content to achieve maximum galvanic performance was 2.00 ± 0.25 mg cm^{-3}. The developed Ni-reinforced metal–metal matrix anodes showed excellent electrochemical characteristics as efficient sacrificial anodes.

Keywords Aluminum · Nickel · Sacrificial anode · Corrosion · Pitting

1 Introduction

Aluminum has been extensively used for making sacrificial anodes owing to its low density, high current capacity and reasonable cost. In neutral noncomplexing solutions, the oxide film on aluminum has very low solubility. Its electronic conductivity is also very low; hence the redox reactions are blocked. Various internal activators such as In, Sn, Bi etc have been used for the activation of aluminum alloy sacrificial anodes [1–5]. Two main explanations have been provided to account for the activation of aluminum; the first involves dissolution of the activator elements from the alloy and their subsequent redeposition on the surface. This process removes the passive film on the Al surface and causes activation [6]. The second explanation is based on the semiconducting properties of the passive film caused by the Sn^{4+} ions. Application of the semiconducting concept is limited only to the Sn activator [7, 8].

Typical internal activators, reported so far, are metals, which have melting points lower than that of aluminum. Even though some studies have been made [9, 10] it remains uncertain whether Ni might activate the aluminum anodes under working conditions. Ni is not generally used as an internal activator material since it has very high melting point. Since the distribution of Ni in the sacrificial anode is not uniform, it is thought that inclusion of Ni may lead to over activation and localized corrosion, resulting in poor efficiency [11]. However in the present work, high performance Al–Zn anodes with incorporated Ni metal particles were developed. Electroless Ni-P plating was done on zinc scrap. The Ni coated Zn scrap was added to the melt before casting the anode. Since the maximum temperature of casting was below 800 °C, Ni was not alloyed but incorporated to the melt as metal particles. The Al–Zn + Ni sacrificial anodes exhibited improved galvanic performance compared to pure Al–Zn alloy sacrificial anodes.

2 Experimental

2.1 Anode casting

Electroless Ni–P plating was carried out on zinc scrap of particle size in the range 500–750 μm. The zinc scrap was mechanically abraded from zinc ingot (99.5%). Ni–P

S. M. A. Shibli (✉) · V. S. Dilimon · A. Mohan
Department of Chemistry, University of Kerala, Kariavattom campus, Trivandrum 695 581, India
e-mail: smashibli@yahoo.com

coating was deposited from a 30 g L^{-1} nickel sulphate + 25 g L^{-1} succinic acid + 25 g L^{-1} sodium hypophosphite bath. The bath pH was kept at a constant value of 4.5 by adding ammonia solution. The plating temperature was maintained at 90 °C. The deposition time was 2 h. EDAX was used to analyze the amount of phosphorous in the sub-monolayer of the Ni–P deposits. The phosphorous content in the deposits was in the range 10–11 at.%.

Al–Zn + Ni anodes were prepared from ultra pure Al (99.99%) and Ni–P coated Zn scrap. Initially, the Al was melted in a muffle furnace. The temperature of the melt was kept at 850 °C for 20 min and the Zn scrap coated with Ni–P was added. The melt was stirred with a silicon carbide rod to obtain a uniform distribution of Zn and Ni. The alloy was poured into a graphite mold of dimension $5 \times 5 \times 0.5$ cm. The anodes were mechanically polished with successively finer grades of emery paper. Finally, the anodes were degreased with trichloroethylene and rinsed with deionized water.

2.2 Physico-chemical evaluations

The hardness of the anodes was analyzed using a Vickers hardness analyzer. A scanning electron microscope (SEM) and energy dispersive X-ray analyzer (EDAX) were used to examine the electrode surface. The pre-treatment of the fresh anode for SEM analysis consisted of etching in 3% NaOH solution. The morphology of the anodes was also studied after they were subjected to accelerated galvanostatic dissolution at a current density of 10 mA cm^{-2}.

The uniform distribution of Ni in the bulk of the anode was checked. A given amount of Al–Zn + Ni anode sample was dissolved in concentrated nitric acid and AAS was used to analyze the amount of Ni in the solution. The measurements were repeated for anode samples taken from different parts randomly selected throughout the bulk of the anode. The results of AAS analysis revealed that the distribution of Ni content was uniform throughout the anode.

2.3 Electrochemical characterization

The Open Circuit Potential (OCP) of the anode was measured as a function of time for 3 months. An electrochemical cell was constructed to determine the efficiency and working potential (or Closed Circuit Potential (CCP)) of the anode. The anode was placed in a specially designed cell, leaving only an area of 10 cm^2 exposed. The cathode was a mild steel sheet of dimensions $11 \times 4 \times 0.5$ cm. During the test the CCP and the cell current were measured as a function of time. The electrolyte was 3% NaCl solution prepared with analytical grade chemicals and distilled water. All potentials were measured relative to a saturated calomel reference electrode (SCE).

The total duration of the long-term electrochemical test was 3 months. At the end of the test, the anodes were removed, cleaned and weighed to obtain the weight loss. The galvanic efficiency of the anodes was obtained by calculating the total charge delivered by the anode, the weight loss of the anode and the corresponding electrochemical equivalent.

$$\text{Efficiency}\,(\eta) = (A/B) \times 100;$$

where A is the actual charge delivered by the anode and B is the theoretical charge corresponding to the observed weight loss.

For polarization studies, a high area platinum counter electrode, Al–Zn + Ni alloy working electrode and SCE reference electrode were used. The Al–Zn + Ni alloy electrodes were fitted in a shrinkable tube and coated with epoxy resin leaving a geometric area of 1 cm^2 exposed. The electrochemical polarization experiments were performed in 3% NaCl, 5% NaCl and 10% NaCl solutions prepared with chemicals of analytical grade and distilled water. The electrochemical studies were carried out at a temperature of 30 ± 1 °C.

3 Results and discussion

3.1 Surface morphology

Figure 1a shows the morphology of the Al–Zn anode, while that of the Al–Zn + Ni anode is presented in Fig. 1b. A significant difference in the morphology of the two anodes is apparent. The Al–Zn + Ni anode has a uniform morphology with smaller and well-refined grains. The grain size and distribution have a large influence on the galvanic performance of the anodes. Generally, anodes with small grains have high current capacity and efficiency [12, 13]. The whole area of Al–Zn anode observed at smaller magnification (Fig. 1a) is more defective than the Al–Zn + Ni anode (Fig. 1b) and displays many voids and cracks. Defective morphology leads to localized corrosion and hence low galvanic efficiency. For the Al–Zn + Ni anode the hardness is remarkably high (Table 2); this is attributable to the presence of Ni and the subsequent morphological and metallurgical improvements.

3.2 Behavior of nickel during anode dissolution

It is important to understand the behavior of the Ni during anode dissolution. The grains and grain boundaries of the fresh Al–Zn + Ni anode observed at higher magnification (Fig. 2a) contain small Ni-rich deposits, but after anodic dissolution for 1 h at a current density of 10 mA cm^{-2}, the surface becomes enriched in Ni (Fig. 2b). Since this study

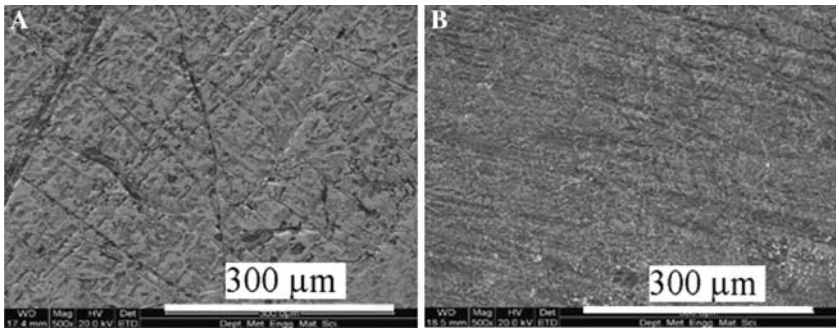

Fig. 1 SEM images showing the surface morphology of (**A**) pure Al–Zn anode and (**B**) Al–Zn + Ni anode

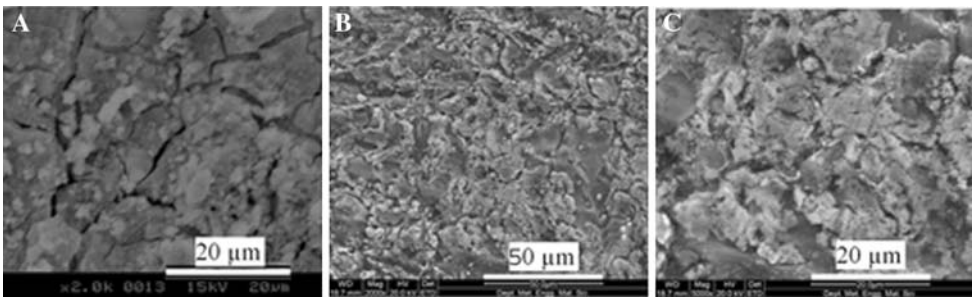

Fig. 2 Change in the surface appearance of the Al–Zn + Ni anodes caused by anodic dissolution for 1 h at a current density of 10 mA cm^{-2}. (**A**) Before anodic dissolution, (**B**) after anodic dissolution, (**C**) magnified view of the surface after anodic dissolution

was carried out under active dissolution conditions (10 mA cm^{-2} anodic current), the enrichment of Ni on the anode surface shows that the deposited Ni interacts with the anode surface. Further anodic dissolution for 1 h causes no change in the Ni content on the anode surface.

In another set of experiments the effect of Ni-rich deposits on the activation of the anode was evaluated. The anodes were galvanostatically polarized in the anodic direction up to a current density of 100 mA cm^{-2} and then the current was interrupted. Sufficient time was then provided for the electrodes to attain stable potential. The repeated polarization curves of Al–Zn and Al–Zn + Ni anodes are shown in Fig. 3. For the Al–Zn + Ni anode, the repetition of polarization (up to 10 cycles) has no effect on the trend and shape of the polarization curves. With reference to Fig. 2, this behavior is attributable to the destruction of the passive alumina film by the Ni deposited on the electrode surface during anodic polarization. Unlike the Al–Zn + Ni anode, the Al–Zn anode displays a completely different behavior during repeated polarization. After four cycles of such polarization and current interruption process, the Al–Zn anode exhibits a rapid rise in potential to the passive region, indicating stable passive film formation.

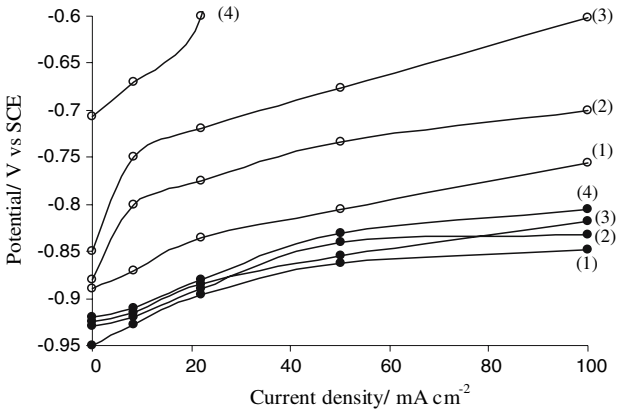

Fig. 3 Comparison of the repeated anodic polarization behavior of Al–Zn and Al–Zn + Ni anodes: (○) Al-Zn anode, (●) Al–Zn + Ni anode. (1) First polarization, (2) second polarization, (3) third polarization, (4) fourth polarization [Electrolyte: 3% NaCl]

3.3 Galvanic performance of the anodes

The galvanic performance of the anodes is compared in Table 1. The Al–Zn + Ni anode exhibits active behavior compared to that of the Al–Zn anode. Active OCP and CCP are desirable because a relatively noble potential indicates passivation. The calculated galvanic efficiency for the Al–Zn + Ni anode was higher (~80%). The galvanostatic anodic polarization curves of Al–Zn and Al–Zn + Ni anodes are displayed in Fig. 4. The polarization curve of the Al–Zn + Ni anode also exhibits active behavior compared to that of the pure Al–Zn anode. The Al–Zn + Ni anode exhibits low polarization and high cathodic potential at all current densities. The trend of the anode potential (OCP) and closed circuit potential against time when the experimental anodes are immersed in different concentrations of NaCl is shown in Figs. 5 and 6. The OCP and CCP of the Al–Zn + Ni anode have more negative values.

Table 1 A comparison of the galvanic performance of the Al + 5% Zn anodes with and without Ni-incorporation

Anode type	Concentration of NaCl medium/%	OCP (V)	Self corrosion $\times 10^{-6}$/g cm^{-2} h^{-1}	Efficiency (%)
Without Ni-incorporation	3	–0.986	9.1857	64
Without Ni-incorporation	5	–0.998	9.5322	62
Without Ni-incorporation	10	–1.020	9.0022	65
With Ni-incorporation	3	–1.021	7.6554	79
With Ni-incorporation	5	–1.039	7.3211	80
With Ni-incorporation	10	–1.065	7.5454	77

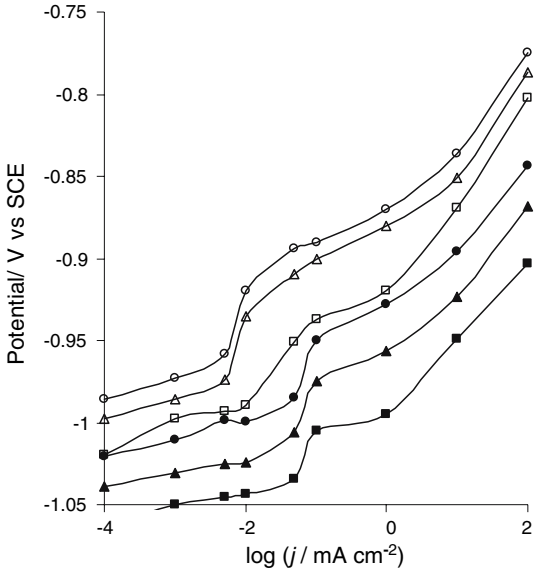

Fig. 4 Comparison of the anodic polarization behavior of Al–Zn + Ni anode with that of pure Al–Zn anode in different concentrations of NaCl solution. (●) Al–Zn + Ni anode in 3% NaCl, (▲) Al–Zn + Ni anode in 5% NaCl, (■) Al–Zn + Ni anode in 10% NaCl, (○) Al–Zn anode in 3% NaCl, (△) Al–Zn anode in 5% NaCl, (□) Al–Zn anode in 10% NaCl

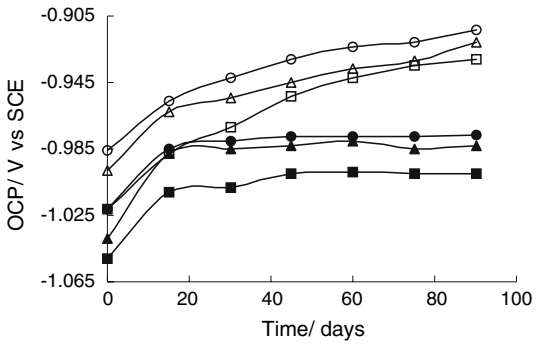

Fig. 5 Variation of OCP of pure Al–Zn anodes and Al–Zn + Ni anodes in different concentrations of NaCl solution. (●) Al–Zn + Ni anode in 3% NaCl, (▲) Al–Zn + Ni anode in 5% NaCl, (■) Al–Zn + Ni anode in 10% NaCl, (○) Al–Zn anode in 3% NaCl, (△) Al–Zn anode in 5% NaCl, (□) Al–Zn anode in 10% NaCl

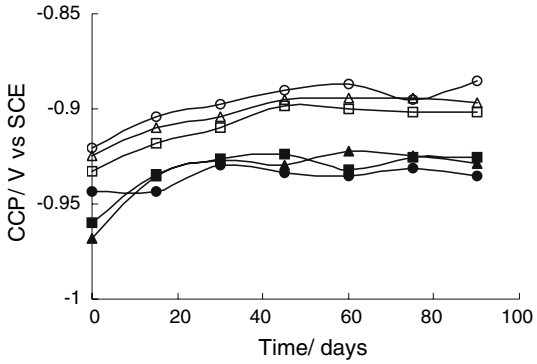

Fig. 6 Variation of CCP of pure Al–Zn anodes and Al–Zn + Ni anodes in different concentrations of NaCl solution. (●) Al–Zn + Ni anode in 3% NaCl, (▲) Al–Zn + Ni anode in 5% NaCl, (■) Al–Zn + Ni anode in 10% NaCl, (○) Al–Zn anode in 3% NaCl, (△) Al–Zn anode in 5% NaCl, (□) Al–Zn anode in 10% NaCl

3.4 Effect of nickel content

The dependence of galvanic performance on the amount of Ni for different types of Al–Zn + Ni anodes is compared in Table 2. The galvanic performance increases with Ni content in the anode up to 2..00 ± 0.25 mg cm^{-3} (corresponding to 5 wt.% Ni-coated Zn in the melt). The reason for this may be the gradual increase in the amount of Ni deposit, which prevents the formation of passive oxide film on the anode surface. Further increase in the Ni content in the anode reduces the galvanic performance. This is due to the increase in the barrier properties of the anode surface due to higher Ni deposition and to the variation of the Zn content from its optimum value of 5 wt.%.

3.5 Chloride ion concentration and pit growth

Corrosion of aluminum is more often governed by pitting rather than uniform corrosion. Al–Zn alloys have been shown to possess more negative pitting potential than Al [14]. As shown in Fig. 7 by increasing the concentration of the NaCl solution from 3% to 10%, the pitting potential of Al–Zn and Al–Zn + Ni anodes shifted to more negative values. However, the pitting potentials are more negative in

Table 2 A comparison of the galvanic performance and physical properties of Al-alloy anodes with different extent of Ni incorporation [Electrolyte: 3% NaCl solution]

Ni-coated Zn in the melt (%)	Ni in the anode (mg cm^{-3})	Hardness/HVN	OCP (V)	CCP/V at different current densities (mA cm^{-2})			Self corrosion $\times 10^{-6}$ (g cm^{-1} h^{-1})	Efficiency (%)
				25	50	100		
2	0.9 ± 0.10	40	–0.969	–0.870	–0.820	–0.765	9.2326	61
4	1.5 ± 0.10	65	–1.005	–0.891	–0.878	–0.825	8.5322	75
5	2.00 ± 0.25	88	–1.021	–0.911	–0.887	–0.844	7.6554	79
6	2.5 ± 0.25	94	–1.008	–0.901	–0.874	–0.811	7.9918	77
8	3 ± 0.25	102	–0.965	–0.869	–0.815	–0.754	9.1232	63

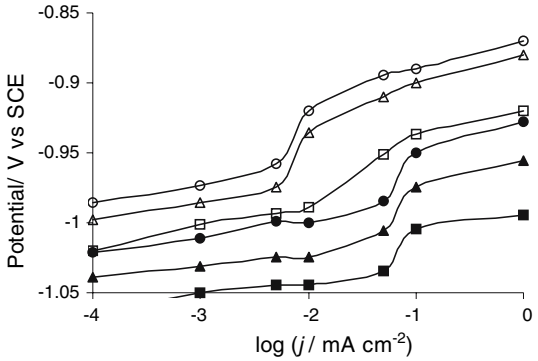

Fig. 7 Variation of pitting potential of Al–Zn anodes and Al–Zn + Ni anodes as a function of electrolyte concentration. (●) Al–Zn + Ni anode in 3% NaCl, (▲) Al–Zn + Ni anode in 5% NaCl, (■) Al–Zn + Ni anode in 10% NaCl, (○) Al–Zn anode in 3% NaCl, (△) Al–Zn anode in 5% NaCl, (□) Al–Zn anode in 10% NaCl

the case of the Al–Zn + Ni anode compared to the Al–Zn anode. The interaction between chloride anions and a passive alumina film can result in adsorption of Cl^- ions on the film, which, in turn, causes film instability and leads eventually to pitting. An increased adsorption of Cl^- is observed at comparatively higher anodic potentials. The areas without a favorable adsorption potential of chloride ions, i.e., more negative than the operating potential, are lost as a passive mass since at this operating potential Cl^- ions cannot effectively adsorb and destruct the passive alumina film to induce corrosion of the anode. The anode materials in these areas are lost as passive mass and not as ions. Such anode mass loss without generation of current results in low anode efficiency. In the present work the Al–Zn + Ni anode possesses a higher negative pitting potential than the Al–Zn anode. At higher chloride concentrations, the surface adsorption of chloride ions initiating pitting becomes effective at high negative potentials. The galvanic performance of the anodes in NaCl solution of different concentrations is also compared in Table 1. The Al–Zn + Ni anode shows higher galvanic performance than the Al–Zn anode in all NaCl solutions.

4 Conclusions

Incorporation of nickel metal into an Al–Zn anode is a convenient method for increasing the galvanic performance of the anode. Al–Zn + Ni anodes have good physico-chemical characteristics. Incorporation of Ni into Al–Zn anodes causes an increase in the galvanic performance. During dissolution of the Al–Zn + Ni anodes in NaCl solution Ni is deposited on the anode surface. The increased activity of Al–Zn + Ni anodes may be attributed to the presence of the Ni deposits and their facility for passive alumina film destruction. For the Al–Zn + Ni anodes the optimum Ni content to achieve maximum galvanic performance is 2.00 ± 0.25 mg cm^{-3}.

Acknowledgments The authors are grateful to the Head of the Department of Chemistry, University of Kerala, for his kind assistance and STEC, Government of Kerala, for financial assistance.

References

1. Saidman SB, Garcia SG, Bessone JB (1995) J Appl Electrochem 25:252
2. Breslin CB, Carroll WM (1992) Corros Sci 33:1735
3. Reboul MC, Gimenez PH, Rameau JJ (1984) Corrosion 40:366
4. Venugopal A, Veluchamy P, Selvam P, Minoura H, Raja VS (1997) Corrosion 53:808
5. Talavera MA, Valdez S, Juarez-Islas JA, Mena B, Genesca J (2002) J Appl Electrochem 32:897
6. Reboul MC, Gimenez PH, Rameau JJ (1984) Corrosion 40:366
7. Keir DS, Pryor MJ, Sperry PR (1967) J Electrochem Soc 114:777
8. Keir DS, Pryor MJ, Sperry PR (1969) J Electrochem Soc 116:319
9. Juchniewicz R, Walaszkowski J, Sokolski W, Stankiewicz E, Bohdanowicz W (1990) Polish patent 152:405
10. Takeuchi H, Ogiwara Y, Shibata N (1998) Japanese patent 10 219, 379
11. Reding JT, Newport JJ (1966) Mater Prot 5(12):15
12. Qi C, Guo Z, Zhang H, Qiu Y, Zhang X (1997) Fushi Kexue Yu Fanghu Jishu 9:231
13. Dung Z, Zhu M, Kong X (2002) Cailiao Baohu 35:8
14. El Shayeb HA, Abd El Wahab FM, Zein El Abedin S (1999) J Appl Electrochem 29:473